Part I
Results

1. Results for the fuel cell

First, a simulation for 8 individuals and 7 generations is performed. Fig 1 shows that the fitness of the best new values hardly changes. Only the fitness of the mean individuals improves on average.
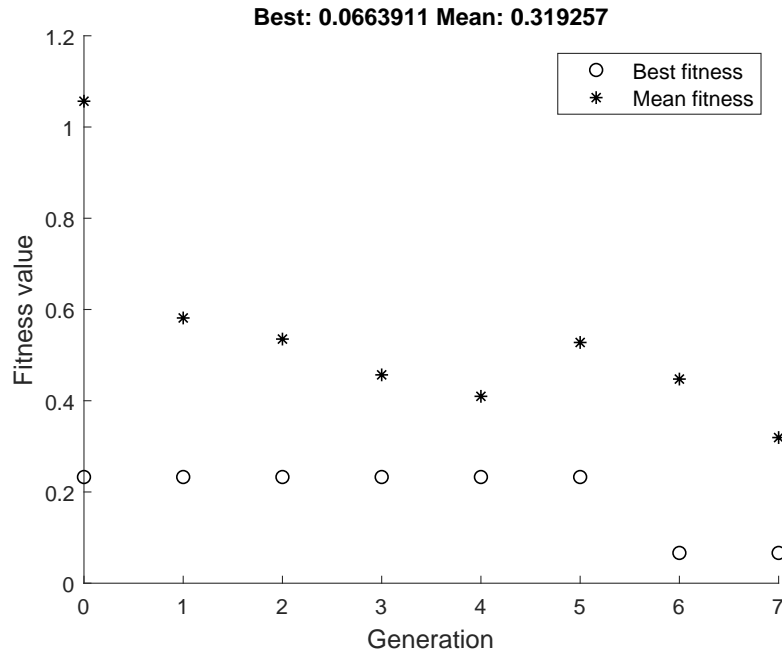

Figure 1: Development of fitness value for a population size of 8 individuals and after 7 generations

As the number of individuals increases, one sees in Fig. 2 that the fitness of the best as well as the bad individuals improves and the performance of average cell power density curve is barely different from the desired result.

Total Output Power

Legend:
- Ideal Curve
- GA Solution

Optimal solution found by
Mixed Integer GA solver:

W = 4.0 mm
Hmem = 30 μm
Hel = 10 μm
ϵ_{cm} = 0.6
λ = 12.0
T = 400 K

X-axis: Current density (A/m^2)
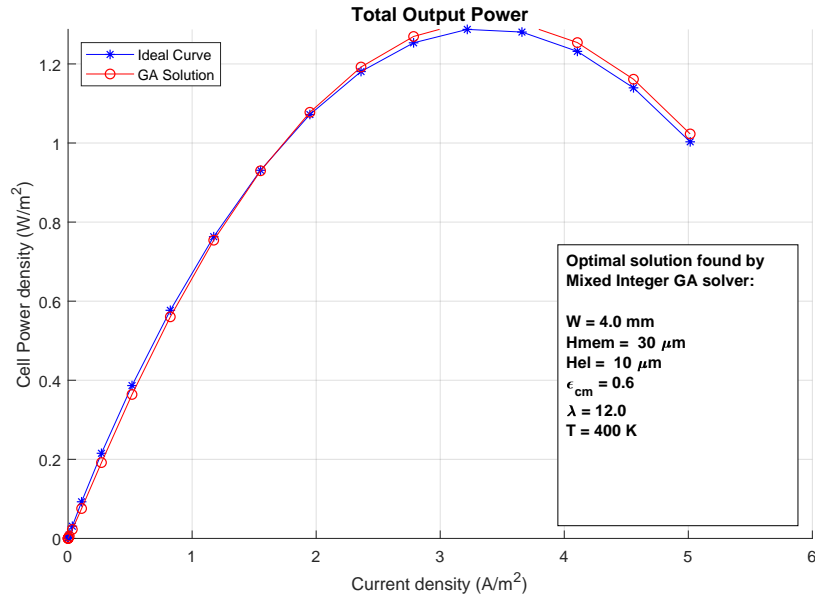Y-axis: Cell Power density (W/m^2)

Figure 2: average cell power density curve

The following figure Fig.3 demonstrates the probabilistic nature of Genetic Algorithms which achieve approximately the same results when choosing different parameters. The solution is therefore not unique. In addition, that means that the desired parameters can be sought out.
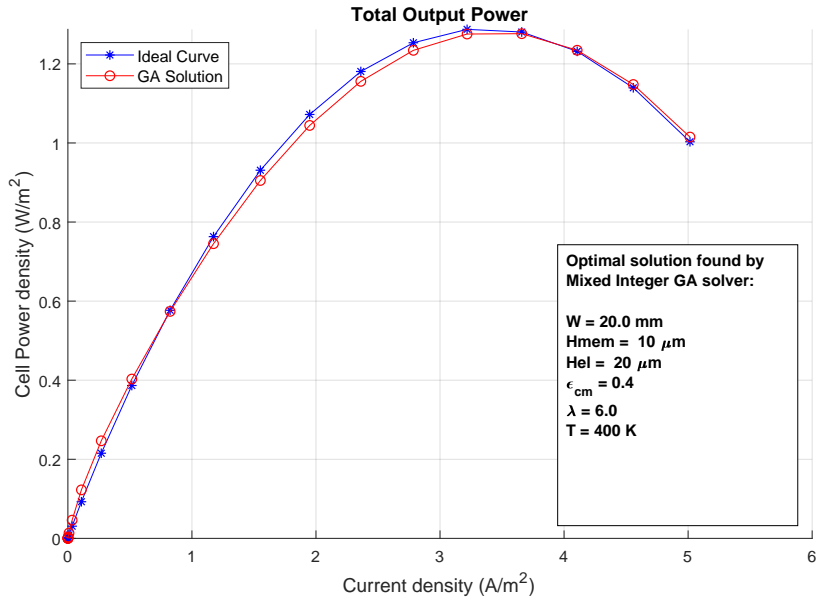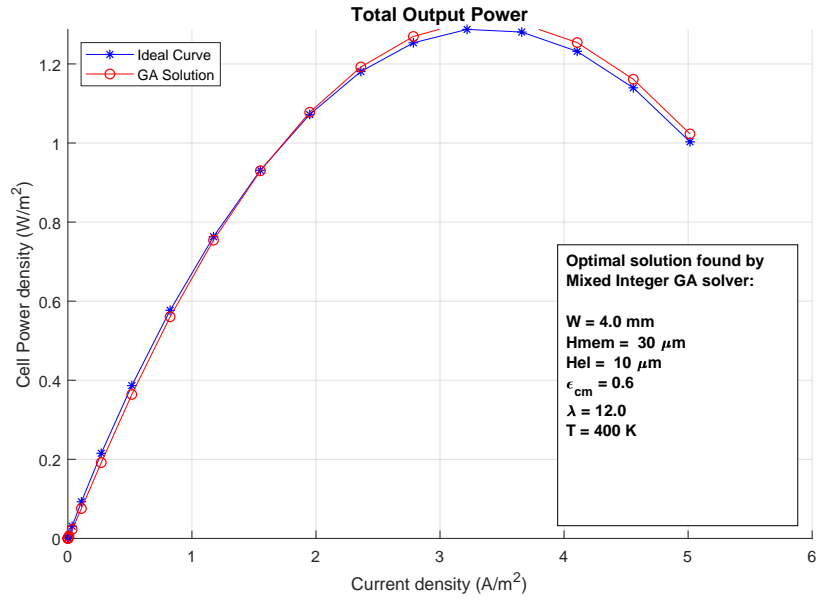
2

Figure 3: The plot shows the non uniqueness of the solution

2. Results for the reverberation chamber

2.1. Result of the optimized stirrer geometry

The objective function that we used is the Shapiro-Wilk-Test value P for the real and imaginary average electric field in each of the three directions in terms of the different parameters

$$F_P = \sqrt{\sum_{i=1}^{6} |P_i\left(tr_1y_1, tr_1y_2, tr_2y_1, tr_2y_2\right) - 1|^2} \rightarrow \min. \tag{1}$$

In order to use a genetic algorithm, a solution space must first be specified. In our case, the following parameters are listed in Table 1 where the range and step size that are necessary for the resolution of the solution space. These values change the shape of the wings.

Table 1: Solution space for genetic algorithms

Symbol	Range		Step size	Unit	Description
tr_1y_1	240	330	9	mm	distance
tr_1y_2	240	330	9	mm	distance
tr_2y_1	10	100	9	mm	distance
tr_2y_2	10	100	9	mm	distance

From the solution space, as shown in Table 1, an initial population is randomly generated. The algorithm improves this population during the simulation until the required criteria is reached.

As the number of individuals increases, Fig. 4 demonstrates that the fitness of the individuals improves and the performance of the distribution is barely different from the desired result.
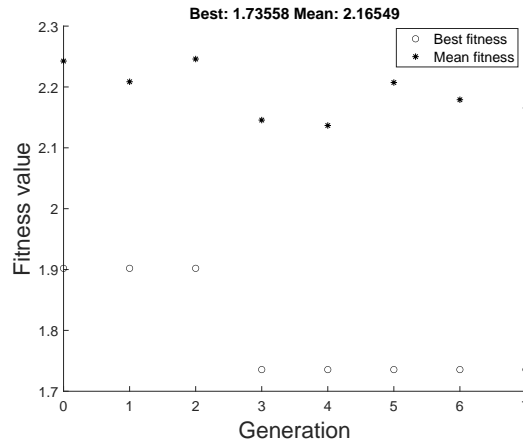

Figure 4: Fitness value of the chosen population size of 18 individuals and 7 generations

The conditions of the run remained the same as for the simulation with the non optimized stirrer geometry. That means that the measurements are taken for 40 stirrer positions and 9 different points spaced out within the chamber. The average value for all points was calculated for both imaginary and real parts in each direction. The distribution of these fields is displayed in Fig.5.
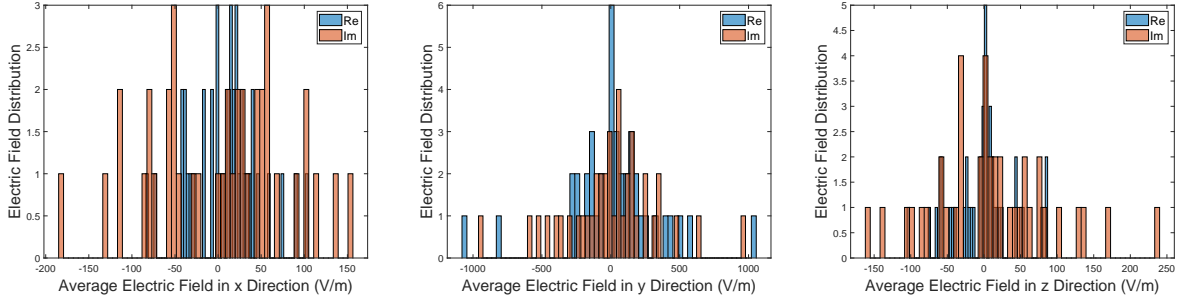

Figure 5: Distribution of the average electric field

The calculation produces the following values for the geometry optimized parameters and P-values for the average electric field distribution.

Table 2: Resulting P-values of the simulation

Symbol	Optimized Values	Unit	Description
tr_1y_1	294	mm	distance
tr_1y_2	28	mm	distance
tr_2y_1	312	mm	distance
tr_2y_2	19	mm	distance

Average Electric Field Distribution	Direction	P-value
Real Part	x	0.4131
	y	0.0019
	z	0.3200
Imaginary Part	x	0.8599
	y	0.1038
	z	0.4860

The P-values from the simulation with the optimized stirrer geometry have improved when compared to the previous simulation but the desired goal has not been reached for all P-values. Therefore, these results lead to the introduction of two more optimized stirrers in remaining x- and y-directions and the optimization of other relevant parameters.
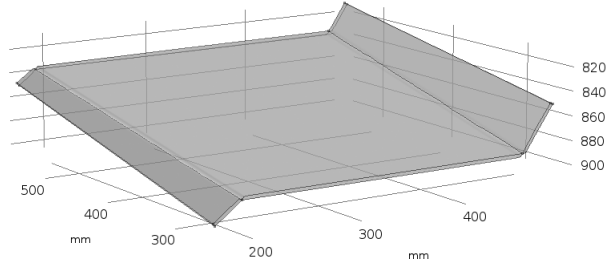
Figure 6: The shape of the optimized stirrer

The Fig. 6 shows the resulting geometry calculated by genetic algorithms.

2.2. Result of the optimized shape for three stirrers

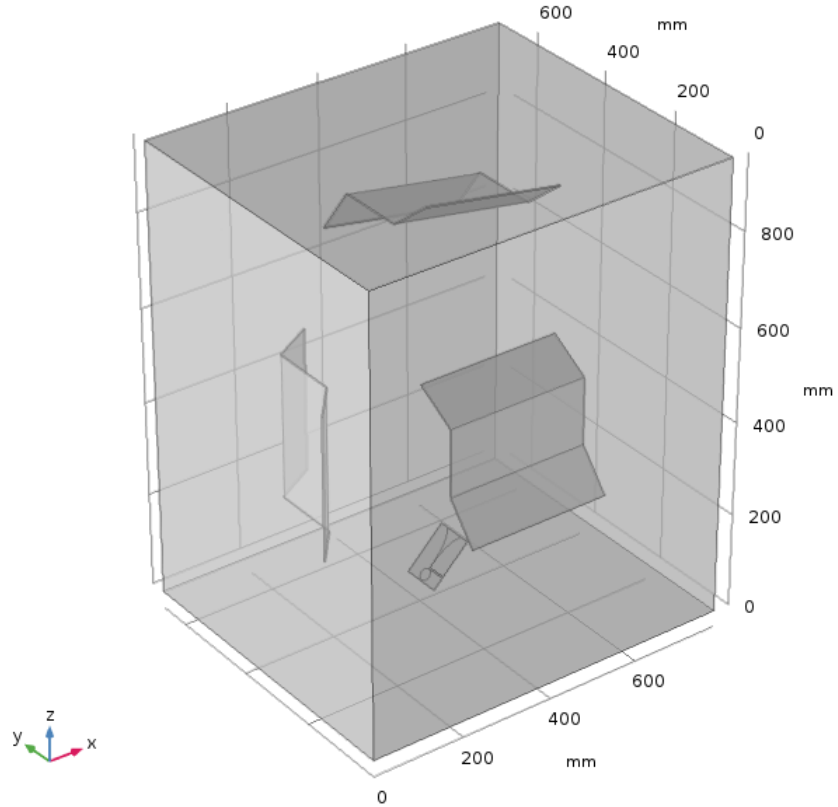In Fig.7, we observe the reverberation chamber with three stirrer whose geometries have will later be optimized.

Figure 7: Setup of the resonance chamber with three stirrers, see Table 3 for their postions

6

The positions of all three stirrers are listed in Table 3.

Table 3: Model parameters and values

Equipment	Parameter	Symbol	Value	Unit
Stirrer 1	Position in x direction	$St_{x,1}$	0	mm
	Position in y direction	$St_{y,1}$	0	mm
	Position in z direction	$St_{z,1}$	860	mm
Stirrer 2	Position in x direction	$St_{x,2}$	0	mm
	Position in y direction	$St_{y,2}$	100	mm
	Position in z direction	$St_{z,2}$	0	mm
Stirrer 3	Position in x direction	$St_{x,3}$	100	mm
	Position in y direction	$St_{y,3}$	0	mm
	Position in z direction	$St_{z,3}$	0	mm

The parameters that have been chosen to be optimized are the shape of the wings for all three stirrers inside the chamber. The newly formulated fitness function for these selected parameters is

$$F_P = \sqrt{\sum_{i=1}^{6} |P_i\left(tr_{11}y_1, ..., tr_{23}y_2\right) - 1|^2} \rightarrow \min. \tag{2}$$

A new solution space for the three stirrers is specified in Table 4.

Table 4: Solution space for genetic algorithms

Equipment	Symbol	Range		Step size	Unit	Description
Stirrer 1	$tr_{11}y_1$	240	330	9	mm	stirrer wing distance 1
	$tr_{11}y_2$	240	330	9	mm	stirrer wing distance 2
	$tr_{21}y_1$	10	100	9	mm	stirrer wing distance 3
	$tr_{21}y_2$	10	100	9	mm	stirrer wing distance 4
Stirrer 2	$tr_{12}y_1$	240	330	9	mm	stirrer wing distance 1
	$tr_{12}y_2$	240	330	9	mm	stirrer wing distance 2
	$tr_{22}y_1$	10	100	9	mm	stirrer wing distance 3
	$tr_{22}y_2$	10	100	9	mm	stirrer wing distance 4
Stirrer 3	$tr_{13}y_1$	240	330	9	mm	stirrer wing distance 1
	$tr_{13}y_2$	240	330	9	mm	stirrer wing distance 2
	$tr_{23}y_1$	10	100	9	mm	stirrer wing distance 3
	$tr_{23}y_2$	10	100	9	mm	stirrer wing distance 4

As previously explained, a population with the chosen size of 18 individuals and 7 generations is generated through the algorithm. Fig. 8 displays the value of the fitness function for each generation.
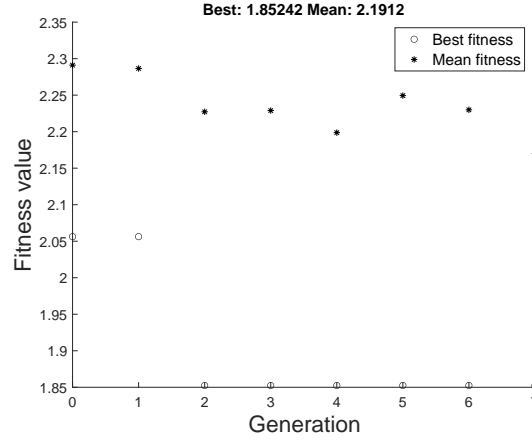

Figure 8: Fitness value of the chosen population size of 18 individuals and 7 generations

The simulation conditions, measurements taken for 40 stirrer positions and 9 different points spaced out within the chamber, remain the same. The histograms on Fig. 9 present the average electric field distribution in all directions for real and imaginary parts.
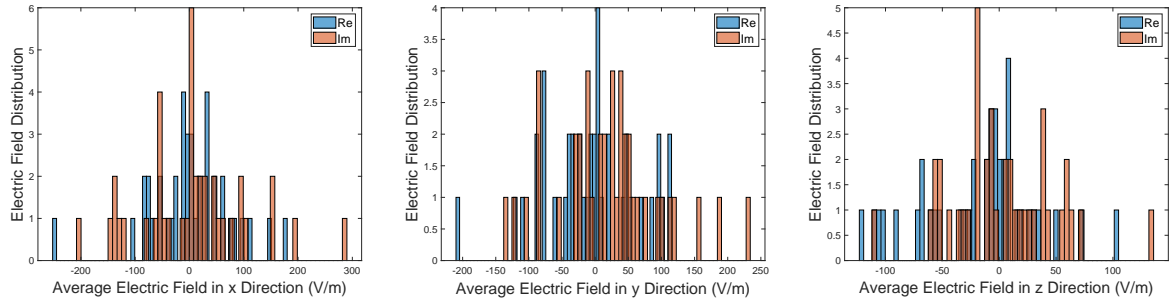

Figure 9: Distribution of the average electric field

Table 5: Resulting P-values of the simulation

Symbol	Optimized Values	Unit
$tr_{11}y_1$	276	mm
$tr_{11}y_2$	240	mm
$tr_{21}y_1$	73	mm
$tr_{21}y_2$	91	mm
$tr_{12}y_1$	276	mm
$tr_{12}y_2$	258	mm
$tr_{22}y_1$	91	mm
$tr_{22}y_2$	28	mm
$tr_{13}y_1$	321	mm
$tr_{13}y_2$	312	mm
$tr_{23}y_1$	64	mm
$tr_{23}y_2$	91	mm

Average Electric Field Distribution	Direction	P-value
Real Part	x	0.0720
	y	0.7291
	z	0.0824
Imaginary Part	x	0.1880
	y	0.4979
	z	0.1378

In conclusion, as seen in Table 5, all resulting P-values have finally fulfilled the desired goal of at least 5% in all directions. This means that, when equiped with three optimised stirrers, the ERC can achieve a normal distribution of the electric field inside the chamber cavity with no further optimizations or changes needed. Of note, is the observation that the optimized stirrers in all cases have favored some symmetrical geometries than initially predicted. This has additionally resulted in stirrers with flater and wider reflective surfaces and smaller stirrer wings.

2.3. Result for using different built-in objects in ERC

The objective function that is used is the Shapiro-Wilk-Test value P for the real and imaginary average electric field in each of the three directions in terms of the different parameters

$$C_P = \sqrt{\sum_{i=1}^{6} |P_i\left(\delta_1 G_1, \delta_2 G_2, ..., \delta_{40} G_{40}\right) - 1|^2} \to \min. \tag{3}$$

where δ_i is an element of a solution space in GA with the value of 0 or 1 and G_i is the specific geometrical object in position i.

Table 6 provides the solution range of the parameters considered for the simulation with genetical algorithms. The x values corresponds to the half spheres where the values 1 and 0 establish whether the geometric object will be switched on or off, meaning that either the half sphere in the given position will be present or erased and, thus, contributing to a different field distribution. The second row supplies Rot that establishes the positions of the stirrer for a full 360 degrees rotation from the simulation in COMSOL Multiphysics. In this case the angular jump corresponds to the number of steps taken by the stirrer.

Table 6: Model parameters for the genetic algorithms and COMSOL Multiphysics simulation

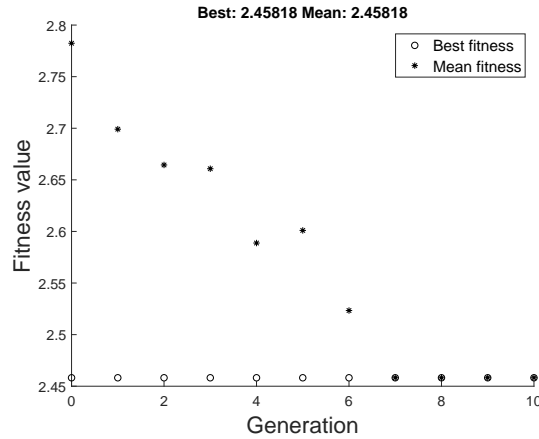| Symbol	Range	Number	Unit	Description
x	$\begin{bmatrix} 0 & 1 \end{bmatrix}$	40	integer	half spheres
Rot	$\begin{bmatrix} 0 & 360 \end{bmatrix}$	60	degrees	rotation positions

Figure 10: Fitness value of the chosen population size of 20 individuals and 10 generations

The ERC with half spheres was simulated for 9 different measurement points inside the chamber and 60 stirrer positions. The histograms on Fig.11 present the average electric field distribution in all directions for real and imaginary parts.
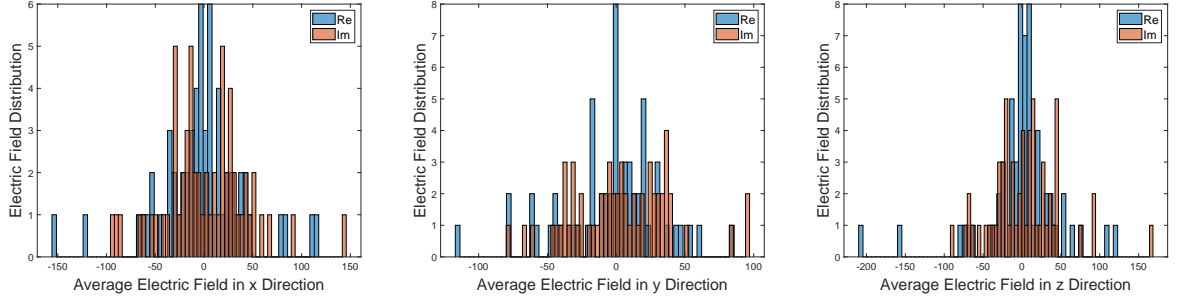
10

Figure 11: Distribution of the average electric field

Resulting from these electric field distributions, the following P-values were determined.

Table 7: Resulting P-values of the simulation

Average Electric Field Distribution	Direction	P-value
Real Part	x	0.4190
	y	0.0182
	z	0.6332
Imaginary Part	x	0.0054
	y	0.5151
	z	0.7989

The P-values from the simulation with the optimized chamber geometry containing half spheres have improved when compared to the previous simulation but the desired goal has not been reached for all P-values. Further simulations are needed to first prove reproducibility and, furthermore, refine the required population size and generations for the genetic algorithms or the stirrer rotation degrees. Moreover, a more important quantity influencing the improvement of the P-values and that should be further honed is the frequency. (These improved simulation will be done these two weeks and the results updated with the improved P-values.)

3. Technical implementation

The GA are implemented in Matlab and thus the initial population is created. The values of the parameters are transmitted to Comsol via Livelink, an interface between Matlab and Comsol. With these values, Comsol simulates the model of the fuel cell and determines the cell current for dierent voltages using finite element method. Matlab get the data through Livelink and calculate the power curve. This is compared with the indicated desired power curve and new values for the parameters are calculated through GA. Finally, the parameters are transmitted to Comsol again and the loop runs until the termination criteria are reached.

11

The calculation time of the implementation is:

$$T_{imp} = n_I * n_G * T_{sim} \tag{4}$$

where n_P is the number of individuals, n_G the number of generations and T_{sim} the time for each simulation. In the mentioned case, the size of the simulation included 8 individuals and 7 generations. A computer with the power of 2.8 GHz CPU and 32 GB RAM was used. For the simulation for fuel cell each simulation lasted in 1 minute and 45 seconds. The total calculation time yielded about 2 hours. The opimization simulation of the optimized stirrer geometry and the performance to optimized the shape of three stirrer yielded about 70 hours. The size of the simulation included 18 individuals and 7 generations. For the simulation of using different built-in objects in ERC there was used 40 individuals and 10 generation and the simulation time was about 2 Weeks. For this simulation in futur work is the parallization of the calculation required